

# Effective Modelling and Simulation of Over-Heated Actuators

M. Zubert<sup>\*</sup>, M. Napieralska<sup>\*</sup>, A. Napieralski<sup>\*</sup>, J.L. Noullet<sup>\*\*</sup>

<sup>\*</sup>Technical University of Lodz, DMCS

Al. Politechniki 11, 93-590 Lodz, Poland, {napier,mnapier,mariuszz}@dmcs.p.lodz.pl

<sup>\*\*</sup>INSA de Toulouse, AIME

135, avenue de Rangueil, 31077 Toulouse Cedex 4, France, noullet@aime.insa-tlse.fr

## ABSTRACT

A mono-dimensional model of an over heated actuator is presented in this paper. The proposed distributed models are derived based on real physical phenomena described by multi-dimensional partial differential equations. The proposed model has been prepared taking into account real polycrystalline silicon parameters and their thermal dependencies. The considerations are based on the previous device analysis and FEM<sup>1</sup> simulation for the device operating in real working conditions in static and quasi-static mode.

**Keywords:** MEMS, over-heated actuator, polycrystalline silicon parameters, mono-dimensional model, RESCUER software

## 1 INTRODUCTION

The paper presents a continuation of work on accurate model of micro-machined over-heated actuator. The previous paper [20] only introduced to a distributed model laying special emphasis on the correct application of boundary conditions and the presentation of chosen simulation results obtained for the considered device performed in the ANSYS simulation environment.

The operating principle of this mechatronic structure (see Figure 1) is based on the coupling between electrical, thermal and mechanical phenomena. The actuator consists of suspended polycrystalline silicon beams. Two of them are anchored to the substrate at the two remaining ends  $\partial\Omega_A$  and  $\partial\Omega_B$  (see cross-sections S1 and S4, Figure 2).

Typical device dimensions: beams length: 30[ $\mu\text{m}$ ], 115[ $\mu\text{m}$ ], 145[ $\mu\text{m}$ ]; beams width 5[ $\mu\text{m}$ ], 20[ $\mu\text{m}$ ]; vertical gap 5[ $\mu\text{m}$ ]; polycrystalline silicon thickness 1.5[ $\mu\text{m}$ ]. When electrical voltage is applied to these terminals, the Joule heat is dissipated in the beams. Since the beam consists of sections having different cross-section area, each section expands thermally differently and as the consequence the actuator bends (see Figure 2,3).

The presented device is relatively simple yet it involves many coupled phenomena having different nature thus it is an excellent example to illustrate multidomain simulation methodology. The mathematical description of the

phenomena occurring in the device and the gradual simplification of the description will be demonstrated in the following sections of the paper.

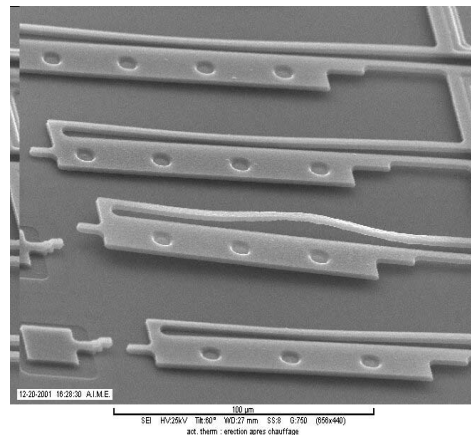


Figure 1 An example of fabricated devices manufactured in the AIME Laboratory.

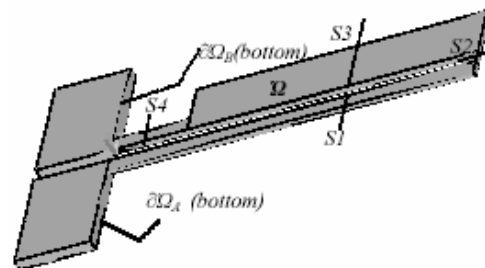


Figure 2 The shape of thermal linear motor [20].

## 2 ELECTRICAL DOMAIN

In the electrical domain, there can be distinguished two electrical terminals (A, B) and a polycrystalline silicon resistor with variable cross-section area. In this case, the electrical phenomena can be simplified and directly described mathematically using lumped network consisting of four resistors connected in series assuming idem

<sup>1</sup> FEM – Finite Elements Method

potential material resistivity, simplified beam join resistances and independence of polycrystalline silicon resistivity on temperature [20]:

$$|j_i| = \frac{I}{S_i}; I = (V_A - V_B) \left( \sum_{k=1}^4 R_k \right)^{-1}; R_k = \rho_{\text{polySi}} \frac{l_k}{S_k} \quad (1a)$$

$$p_{\text{th},i} = \rho_{\text{polySi}} \cdot (I/S_i)^2 \quad (1b)$$

where  $I$  – device current,  $R_k$  – lumped beam resistance;  $S_i$ ,  $l_k$  – cross-section area and length of the beam (for  $R_k$ ) respectively;  $j_i$  – the current density in  $R_k$ ,  $V_A, V_B$  – voltage applied to electrical terminals **A** and **B** respectively;  $I, k$  – the cross-section number (see  $S_i$  in Figure 2);  $p_{\text{th},i}$  – thermal power density of dissipated heat in  $R_k$ ,  $\rho_{\text{polySi}}$  – polycrystalline silicon resistivity.

### 3 THERMAL DOMAIN

Fortunately, the coupling between electrical, thermal and mechanical phenomena allows the assumption of unidirectional power transfer from electrical to thermal domain and after that to mechanical one. Therefore a quasi-static thermal model can be adopted and consequently the thermo-dynamic coupling of the mechanical and thermal domain can be neglected in the heat transfer equation. Additionally, assuming homogeneous distribution of temperature in the device cross-section, the thermal phenomena can be modelled using the mono-dimensional form [20]:

$$\begin{cases} \partial_\xi (\lambda(\xi) \partial_\xi T(\xi)) + p_{\text{th}}(\xi) = h(\xi) \cdot (T(\xi) - T_{\text{ext}}) \\ \text{for } \xi \equiv (\mathbf{x}, \mathbf{y}) \in \Omega; \\ T(\xi) = T_{\text{ext}} \\ \text{for } \xi \equiv (\mathbf{x}, \mathbf{y}) \in \partial\Omega_A \cup \partial\Omega_B \end{cases} \quad (2a)$$

where  $T(\xi)$  – unknown temperature along particular beam in Kelvin degree (!);  $h(\xi)$  – heat transfer coefficient;  $\lambda$  – thermal conductivity;  $T_{\text{ext}}$  – air temperature in Kelvin degree;  $\xi$  – “the natural coordinate” from the terminal **A** to **B**;  $\partial\Omega_A$  and  $\partial\Omega_B$  – the contacts of electrical terminals (**A** and **B**);  $\partial\Omega = \partial\Omega_A \cup \partial\Omega_B \cup \partial\Omega_C$ ,  $p_{\text{th}}(\xi) = p_{\text{th},i(\xi)} \cdot S_{i(\xi)}$  etc

Then, the nonlinearity of equation (2) can be removed from the differential operator by assuming that the thermal conductivity can be approximated by the following expression (for more see section 5):

$$\lambda(\xi) = \lambda_0(\xi) T(\xi)^{\lambda_1(\xi)} \Rightarrow \hat{T}(\xi) = \frac{\lambda_0(\xi)}{\lambda_1(\xi) + 1} T(\xi)^{\lambda_1(\xi) + 1} + C_1 \quad (2b)$$

where  $\hat{T}(\xi)$  – transformed temperature value;  $C_1$  – constant parameter, we will assume that  $C_1 = 0$ .

$$\begin{cases} \partial_{\xi, \xi} \hat{T}(\xi) + p_{\text{th}}(\xi) = h(\xi) \cdot \left( \lambda_1(\xi) + 1 \sqrt{\hat{T}(\xi)} \cdot \varsigma - T_{\text{ext}} \right) \\ \text{for } \xi \equiv (\mathbf{x}, \mathbf{y}) \in \Omega; \\ T(\xi) = T_{\text{ext}} \\ \text{for } \xi \equiv (\mathbf{x}, \mathbf{y}) \in \partial\Omega_A \cup \partial\Omega_B \end{cases} \quad (2c)$$

$$\text{where } \varsigma = \lambda_1(\xi) + 1 \sqrt{\frac{\lambda_1(\xi) + 1}{\lambda_0(\xi)}}.$$

The detailed analysis shows that Raleigh number for the air flow in the air gap between two polycrystalline silicon walls (beams S1 – beam S3 and beam S1 – beam S4) is quite small  $(Ra)_{l=5[\mu\text{m}]} \cong 85.73$  and consequently the heat transfer between walls can be approximated using the Fourier law<sup>2</sup> as follows:

$$\mathbf{q} \cong \frac{\lambda_{\text{air}}}{\delta} \Delta T \quad (3)$$

where  $\Delta T$  – wall temperature difference,  $\lambda_{\text{air}}$  – air thermal conductivity;  $\delta$  – distance between walls;  $\mathbf{q}$  – thermal flux. This phenomenon can be taken into account as an additional heat source increasing  $p_{\text{th}}(\xi)$ . In this case the heat transfer coefficients  $h(\xi)$  have been estimated as the combination of Nusselt number for the whole beam [1] and vertical beam side (for more see [20]).

$$\begin{aligned} h(\xi) \cong & \left[ d^{*5/4} \alpha 0.372 \cdot \left( \frac{\nu/a}{0.7} \right)^{1/4} - \right. \\ & \left. t^{5/4} (\alpha - 1) 0.6773 \left( \frac{\nu/a}{(\nu/a) + 0.952} \right)^{1/4} \right] \cdot \\ & \frac{g \lambda_{\text{air}} (T_{\text{ext}})}{\nu^2 T_{\text{ext}}} (T(\xi) - T_{\text{ext}})^{1/4}; \end{aligned} \quad (4)$$

$$d^* = \frac{w(\xi) + t}{2}; \alpha = \frac{t}{2w(\xi) + t} + 1$$

where  $\nu$  – coefficient of air kinematics viscosity,  $a$  – air thermal diffusivity;  $w(\xi)$  – beam width;  $t$  – beam thickness.

<sup>2</sup> It takes into consideration only static phenomena. The values of air and polycrystalline silicon thermal compensation coefficients are bound by the relation  $a_{\text{polysilicon}} \approx 2a_{\text{air}}$ , where  $a = \lambda / (c\delta)$ , hence the thermal response in these materials are comparable. In other words “temperature covers twice as much distance in polycrystalline silicon as in air at the same time” ( $x_{\text{air}} \approx 2x_{\text{polysilicon}}$ ). Fortunately this effect can be neglected due to the difference in air and polycrystalline silicon thermal conductivities ( $\lambda_{\text{polysilicon}} \approx 350\lambda_{\text{air}}$ ).

#### 4 MECHANICAL DOMAIN

The considered device consists of two non-equally heated beams. The device dimensions and thermal diffusivity allows the adoption of a non-isothermal large deflection model (form more see [2]-[5]) using modified Bernoulli-Euler equation [20].

$$\frac{d\varphi(\xi)}{ds} \equiv (1 - \beta(T(\xi) - T_0(\xi)))^{-1} \frac{M(\xi)}{EJ} \quad (5a)$$

$$\frac{d\varphi(\xi)}{ds} = -\frac{d^2y(x)}{dx^2} \left( 1 + \left( \frac{dy(x)}{dx} \right)^2 \right)^{-3/2} \quad (5b)$$

$$S(\xi) \rho_{polySi} \frac{\partial^2 y(\xi, t)}{\partial t^2} = \frac{\partial^2 M(\xi, t)}{\partial \xi^2} - N \frac{\partial^2 y(\xi, t)}{\partial \xi^2} \quad (5c)$$

where  $s$  – natural co-ordinate  $s \in \langle 0, L \rangle$ ;  $L$  – beam length;  $\varphi = \varphi(\xi) = \arctan \partial_{xy}(x)$  – the bending angle of the beam ( $\partial_{\xi} \varphi(\xi) = R^{-1}$ );  $J$  – beam inertial moment,  $y(\xi)$  and  $M=M(\xi)$  – beam bending and mechanical moment at point  $s$  respectively (see Figure 3);  $E$  – Young modulus;  $\nu$  – Poisson coefficient;  $\beta$  – thermal expansion coefficient;  $N$  – force associated with stress generation an axial force.

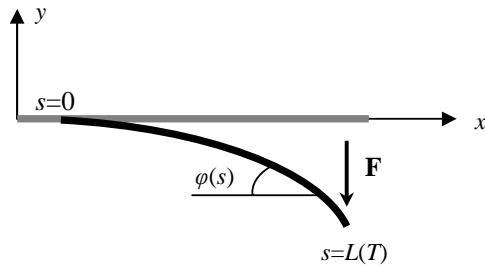


Figure 3 The schematic draft of large deflected beam

#### 5 MATERIAL PROPERTIES

The most of the micro-machined elements similar to the presented micro-actuator are realized using polycrystalline silicon. Unfortunately, not all thermal and mechanical properties of this material have similar values to the bulk silicon properties. On the other hand, the thermal parameter dependence has to be taken into account for large temperature variation. Therefore, polycrystalline silicon parameters estimation will be presented in the next section.

The following investigation procedure and final approximation of polycrystalline silicon thermal properties in the temperature range between 250 K and 1200 K will be proposed for their lack in the professional literature.

In most cases, the silicon thermal conductivity is represented using only the first term of Taylor expansion. This approach is accurate inside a particular neighbourhood of an expansion point, but cannot be accurate for the large temperature variation range. A simple analysis of the experimental data [10]-[12] shows that the power approximation of the thermal conductance can be described

for the temperatures between 250 K and 1200 K by the below expressions proposed by the authors:

$$\lambda_{Si}(T) \equiv 2533.25_{-573.18}^{+740.79} T^{-1.29697_{-0.03941}^{+0.03941}} \left[ \frac{W}{cm \cdot K} \right] \quad (6a)$$

$$D_{Si}(T) \equiv 4269.39_{-1968.79}^{+3653.64} T^{-1.49425_{-0.09652}^{+0.09653}} \left[ cm^2 / s \right] \quad (6b)$$

The thermal conductivity of polycrystalline silicon is reduced by the phonon grain boundary scattering effect [14]. This phenomenon is similar to the electrical resistance of segmented conductor or magnetic resistance of segmented ferromagnetic materials in an electro-magnetic field and similarly depends on the grain size. Its size and particular grain conductivity depends on grain localization, poly-silicon element thickness [13], material doping [14] and deposition pressure and temperature [16]. In the case of undoped polycrystalline silicon layers the thermal conductivity can be effectively approximated by the following expression (the experimental measurements for temperatures between 250 K and 300 K have been taken from [13]):

$$\lambda_{polySi}(T) \equiv 15.0257_{-11.4579}^{+48.2547} T^{-0.738631_{-0.004382}^{+0.004381}} \left[ \frac{W}{cm \cdot K} \right] \quad (7a)$$

The proposed approximation can be also used for the extrapolation of polysilicon behaviour up to critical temperatures of 1150 K, (see also [15]). Additionally, assuming the same density and specific heat, the thermal diffusivity can be approximated by the following form:

$$D_{polySi}(T) \equiv \frac{k_{polySi}(T)}{k_{Si}(T)} D_{Si}(T) \equiv 25.3234 T^{-0.935911} \left[ cm^2 / s \right] \quad (7b)$$

The temperature dependence of the linear expansion coefficient can be approximated by the following expression using silicon measurement data (the experimental measurements have been taken from [17]):

$$\begin{aligned} \beta_{polySi}(T) \approx \beta_{Si}(T) = & -0.257366_{-0.41062}^{+0.41062} + \\ & + 13.0489_{-1.95453}^{+1.95453} \times 10^{-3} T + \\ & + 12.8971_{-2.72858}^{+2.72858} \times 10^{-6} T^2 + \\ & + 4.3542_{-1.1517}^{+1.1517} \times 10^{-9} T^3 \left[ 10^{-6} K^{-1} \right] \end{aligned} \quad (7c)$$

The approximation of electrical resistivity will be taken from the paper<sup>3</sup> [15]

$$\begin{aligned} \rho_{polySi}(T) \approx & 8.(3) \cdot \left( 1 + 9.1 \times 10^{-4} (T - 300) + \right. \\ & \left. + 7.9 \times 10^{-7} (T - 300)^2 \right) \left[ \mu\Omega \cdot m \right] \end{aligned} \quad (7d)$$

Other applied parameter values, e.g. material density, have been assumed to be equal to the bulk silicon ones.

$$\delta_{polySi} \approx \delta_{Si} = 2.329 \left[ g / cm^3 \right] \quad (8)$$

<sup>3</sup> The electrical conductivity depends on grain size.

As it was written before, the polycrystalline silicon parameters are dependent on the grain and element size and the deposition process parameters. Therefore, the research literature reports a Young's modulus ranging between 140 GPa and 210 GPa [19]. The value 165 GPa will be the most appropriate [16].

## 6 CONCLUSIONS

The paper presents an approach to the over heated actuator modelling taking into account its real behaviour. It requires the use of real values of polycrystalline silicon parameters and their thermal dependences. The modelling of such devices, despite their simplicity, is quite a difficult task because of the coupled multidomain phenomena occurring in the device. The proposed model can be implemented using the RESCUER language [6]-[8] and translated to the SPICE simulation environment. The final implementation of the complex model should additionally take into account both the dynamic model response and technological parameter distribution.

## 7 ACKNOWLEDGEMENT

The work reported in this paper was supported by the Internal University Grant K-25/1/2003-Dz.S.

## REFERENCES

- [1] R. Herman. Wärmeübergang bei freier Strömung am waagerechten Zylinder zweiatomigen Gasen. VDI – Forschungsheft nr 379, Berlin 1936
- [2] L. D. Landau and E. M. Lifshitz, Theory of Elasticity 3rd Rev. Edit. Butterworth-Heinemann, February 1995 (Pergamon, 1975)
- [3] S. Timoshenko Theory of Elasticity. 3rd edition McGraw Hill College, June 1970
- [4] J. V. Clark, D. Bindel, W. Kao, E. Zhu, A. Kuo, N. Zhou, J. Nie, J. Demmel, Z. Bai, S. Govindjee, K. S. J. Pister, M. Gu, A. Agogino, "Addressing the Needs of Complex MEMS Design." To appear in MEMS 2002. L.V., Nevada, Jan, 2002.
- [5] P. Allen, J. Howard, E. Kolesar, J. Wilken. "Design, Finite Element Analysis, and Experimental Evaluation of a Thermal-Actuated Beam Used to Achieve Large In-Plane Mechanical Deflection". Tech Digest. Solid-state Sensor and actuator workshop, Hilton Head Island SC, pp.191-196, June 8-11, 1998
- [6] Zubert M., Napieralski A.: "RESCUER – The revolution in multidomain simulations – Part I and II", Proc. 22nd International Conference on Microelectronics (MIEL2000), Niš, Serbia, 14-17 may 2000, vol.2 , pp. 549-559
- [7] M. Zubert, M. Napieralska, A. Napieralski. "RESCUER – The new solution in multidomain simulations", Elsevier, Microelectronics Journal 31 (11-12) (2000) pp. 945-954
- [8] M. Zubert, A. Napieralski, M. Napieralska. „The Application of RESCUER Software to Effective MEMS Design and Simulation”, *Bulletin of the Polish Academy of Sciences – Technical Science*, No. 4, Warsaw, November 2001
- [9] J. V. Clark, at all, "Sugar: Advancements in a 3D Multi-Domain Simulation Package for MEMS". In *Proc. of the Microscale Systems: Mechanics and Measurements Symposium*. Portland, OR, June 4, 2001
- [10] B. Abeles, D.S. Beers, G.D. Cody, J.P. Dismukes. *Phys. Rev. (USA)* vol.125 (1962) p.44
- [11] P. Turkes. *Phys. Status Solidi A* (Germany) vol.75 no.2 (1983) p.519-23
- [12] C.J. Glassbrenner, G.A. Slack. *Phys. Rev. (USA)* vol.134 (1964) p.A1058
- [13] S. Uma A.D. McConnell M. Asheghi K. Kurabayashi and K.E. Goodson. "Temperature dependent thermal conductivity of undoped polycrystalline silicon layers". *14<sup>th</sup> Symposium on Thermophysical Properties*, Boulder, Colorado, U.S.A., June 25-30, 2000
- [14] M. Asheghi, K. Kurabayashi, R. Kasnavi, K. E. Goodson. "Thermal conduction in doped single-crystal silicon films". *Journal of Applied Physics*. Vol. 91, No 8, 15 April 2002, pp. 5079-5088
- [15] S. Holzer, R. Minixhofer, C. Heitzinger, J. Fellner, T. Grasser, S. Selberherr "Extraction of Material Parameters Based on Inverse Modeling of Three-Dimensional Interconnect Structures". *9<sup>th</sup> THERMINIC Workshop*, 24-26 Sep. 2003, Aix-en-Provence, France, pp. 263-268
- [16] "MEMS Reliability Assurance Guidelines for Space Applications", NASA, *Jet Propulsion Laboratory Publication 99-1*, California, January 1999
- [17] Okada, Y. and Y. Tokumaru, *J. Appl. Phys.* **56**, 2 (1984) 314-320.
- [18] R. Hull. "Properties of Crystalline Silicon", *INSPEC*, London, 1999
- [19] D. W. Burns, *Micromechanics of Integrated Sensors and the Planar Processed Pressure Transducer*, Ph.D. Thesis, University of Wisconsin, Madison, 1988.
- [20] M. Zubert., M. Napieralska., A. Napieralski, J.L. Noullet: "Generation of Reduced Models for Over-Heated Actuators. Multidomain Simulation Program". ", *Proceedings of the 9<sup>th</sup> International Conference "Mixed Design of Integrated Circuits and Systems" MIXDES'2002*, Wrocław, Poland 20-22 June 2002, pp. 435-440